Secondary pulmonary lymphoma diagnosed by minimal residual disease detected in bronchoalveolar lavage fluid: A case report

YINGYING HU[1,2*], ZHENG LV[1,2*], LEHAO REN[1,2], XIN ZHAO[1,2], HONG LIU[1,2] and YIN YUAN[1,2]

[1]Department of Critical Care Medicine, Union Hospital, Tongji Medical College, Huazhong University of Science and Technology, Wuhan, Hubei 430022, P.R. China; [2]Institute of Anesthesia and Critical Care Medicine, Union Hospital, Tongji Medical College, Huazhong University of Science and Technology, Wuhan, Hubei 430022, P.R. China

Received June 17, 2025; Accepted January 7, 2026

DOI: 10.3892/etm.2026.13109

Abstract. The present study reports 2 cases of non-Hodgkin's lymphoma (NHL) that achieved complete remission following cyclophosphamide, hydroxydaunorubicin (doxorubicin), oncovin (vincristine) and prednisone chemotherapy. Both patients subsequently developed respiratory distress and rapid progression. The initial diagnosis was pulmonary infection, based on the symptoms of cough, white sputum and fever, abnormal laboratory results of high white blood cells, C-reactive protein and procalcitonin and most notably, chest CT scans showing ground-glass opacities and patchy shadows. Following treatment with a number of antibiotics, the pulmonary symptoms of the patients and their imaging manifestations improved at first. The repeated negative results of sputum culture and next-generation sequencing of bronchoalveolar lavage fluid (BALF) confirmed that the pathogens were eliminated. However, later, the symptoms and signs of both patients continued to progress. Secondary pulmonary lymphoma was not confirmed until the discovery of lymphocytes with abnormal phenotypes following minimal residual disease (MRD) testing in BALF. Both patients ultimately succumbed to respiratory failure. The present report outlines the first 2 reported cases of NHL diagnosed through MRD detection in BALF alongside a review of the relevant literature.

Introduction

The occurrence of secondary pulmonary lymphoma (SPL) in patients diagnosed with non-Hodgkin's lymphoma (NHL) is not rare. Apart from the gastrointestinal tract, the lungs are one of the most frequent extra-nodal sites invaded by NHL, with 25-40% reported in the literature (1,2). SPL is part of systemic lymphoma and can invade lung tissue through blood dissemination or transfer to the lung through hilar and mediastinal lymph nodes. Clinically, patients frequently present with an occasional cough and hemoptysis, the same symptoms as those of pneumonia (3). Therefore, when CT scans demonstrate pneumonia-like imaging features, distinguishing between SPL and infectious pneumonia poses notable diagnostic challenges. The risk of opportunistic infections is influenced by the degree of pathogen exposure, host immune status and pathogen-host interactions (4). Patients with hematologic malignancies are prone to pulmonary opportunistic infections, which often deteriorate rapidly and evolve into respiratory failure (5). However, diagnosis is often delayed and occasionally completely overlooked, especially with invasive bronchopulmonary aspergillosis. The commonly used diagnostic methods for SPL include transbronchial lung biopsy or CT-guided lung biopsy and surgical interventions. The present report outlines 2 cases of coexistent SPL and opportunistic infections in patients with NHL diagnosed by minimal residual disease (MRD) detected in bronchoalveolar lavage fluid (BALF), as well as a review of the relevant literature.

Case report

Case 1. A 63-year-old woman with no past medical history of lymphoma was diagnosed with peripheral T cell lymphoma following a skin biopsy within the Department of Dermatology (Union Hospital, Tongji Medical College, Huazhong University of Science and Technology, Hubei, China), based on the symptoms of a skin rash and pruritus 1 year prior to admission in October 2024. The patient completed six cycles of 100 mg thalidomide + 50 mg/m^2 etoposide + 750 mg/m^2 cyclophosphamide + 50 mg/m^2 hydroxydaunorubicin + 1.4 mg/m^2 vincristine sulfate + 100 mg prednisone, and acquired complete remission 2 months prior to hospitalization. Furthermore, 20 days before admission to the Department of Critical Care Medicine, the patient was diagnosed with a pulmonary infection and received 6 days of mechanical ventilation due to severe respiratory failure. Following combination treatment with antibiotics, the patient was successfully weaned and discharged. Subsequently,

Correspondence to: Professor Yin Yuan, Department of Critical Care Medicine, Union Hospital, Tongji Medical College, Huazhong University of Science and Technology, 1,277 Jiefang Avenue, Wuhan, Hubei 430022, P.R. China
E-mail: simiyy721@163.com

*Contributed equally

Key words: secondary pulmonary lymphoma, pulmonary infection, bronchoalveolar lavage fluid, biopsy, minimal residual disease

1 week later, the patient was re-admitted, presenting with a worsening cough, white sputum and an intermittent fever (maximum of 39.4˚C). Compared with the complete blood count 1 week ago, the white blood cell count of the patient was higher ($201.57x10^9$/l; normal range, 3.5-$9.5x10^9$/l), with 84.2% lymphocytes. Additionally, results of liver and kidney function, coagulation function and echocardiography appeared similarly normal compared with 1 week ago. Chest CT scans revealed enlarged consolidation, segmental atelectasis and mediastinal lymph nodes (Fig. 1A-D). The patient therefore received mechanical ventilation, due to respiratory failure and empirical anti-infection treatment with cefoperazone sodium and sulbactam sodium. Simultaneously, the patient underwent bronchoscopy and bronchoalveolar lavage, which revealed thin, white secretions. BALF was sent for metagenomic next-generation sequencing (mNGS) (Table SI), revealing the presence of human γ-herpesvirus 4 (sequence no. 118) and *Streptococcus pneumoniae* (sequence no. 15) which did not align with clinical symptoms or CT findings. Meanwhile, to rule out bloodstream infection, peripheral blood specimens were also collected and sent for mNGS testing. The results revealed that 217 sequences of Torque teno virus and 160 sequences of human β-herpesvirus 6B were detected.

The patient did not undergo CT-guided percutaneous lung biopsy due to coagulation dysfunction, but BALF was tested to detect MRD and malignant cells were identified by abnormal immunophenotypic molecules. The BALF MRD test results revealed that 94.21% karyocytes were lymphocytes and matured γδ T cells accounted for 20.91% karyocytes exhibiting the phenotypes $CD3^+$, $CD5^+$, T cell receptor (TCR)-$\gamma\delta^+$, TCR $V\delta1^+$, $CD4^-$, $CD8^-$, $CD7^-$ and TCR$\alpha\beta^-$ (Fig. 2), consistent with the immunophenotypic profile observed in bone marrow (Fig. 3) and peripheral blood samples (Fig. 4) from peripheral T cell lymphoma. Until then, the patient had been diagnosed with SPL and accordingly, had received methylprednisolone (80 mg/day) and responded well. The oxygenation index of the patient had markedly improved and the white blood cells count had notably decreased. CT scans showed that the lung disease was locally alleviated (Fig. 1G and H). The patient was successfully extubated on day 8 of mechanical ventilation. However, the patient declined further antitumor treatment. Eventually the respiratory failure continued to progress, leading to mortality 20 days later.

Case 2. A 59-year-old man was diagnosed with follicular lymphoma 6 years prior to the present hospitalization and achieved complete remission following six cycles of rituximab CHOP chemotherapy. The patient then received single-drug maintenance therapy with rituximab. No follow-up treatment was conducted in the previous 4 years before admission to the Department of Lymphoma of Union Hospital (Tongji Medical College, Huazhong University of Science and Technology, Hubei, China) in November 2024 with systemic lymph node enlargement. The neck lymph node and bone marrow biopsy both showed lymphoma infiltration. A regimen of 10 mg/m^2 dexamethasone, 500 mg/m^2 cyclophosphamide and 90 mg/m^2 bendamustine were administered as antitumor treatment. After 1 week, the patient exhibited sudden respiratory distress with decreased blood oxygen saturation (minimum 68%) and moist rale at the bottom of the lung. The patient was then transferred to the intensive care unit for further management, including mechanical ventilation. Laboratory test results revealed a white blood cell count of $134.80x10^9$/l with 16.42% neutrophils, 81.4% lymphocytes, 0.45% basophils, 0.22% eosinophils, 1.48% monocytes, an erythrocyte count of $3.03x10^{12}$/l (normal range, 3.8-$5.1x10^{12}$/l) and a platelet count of $128x10^9$/l (normal range, 125-$350x10^9$/l). The C-reactive protein level was 96.60 mg/l (normal range, 0-4 mg/l), procalcitonin (PCT) was 4.32 ng/ml (normal range, 0-0.5 ng/ml) and lactate dehydrogenase was 203 U/l (normal range, 109-245 U/l).

The initial sputum culture was extended-spectrum β-lactamase (+), *Escherichia coli* and the sputum mNGS revealed *Moraxella catarrhalis* (sequence no. 134), *Pneumocystis jiroveci* (sequence no. 4) and Torque teno virus (sequence no. 50). In addition, cytomegalovirus presence in whole blood cells was negative whereas the Epstein-Barr virus was positive (copy no. $6.82x10^3$). Chest CT scans (Fig. 5A and B) showed large areas of ground-glass opacity and patchy shadows. The patient was further diagnosed with pulmonary infection and received empirical treatment with 1,000 mg meropenem every 8 h, 50 mg caspofungin every day, 15 mg/kg trimethoprim/sulfamethoxazole every day and 5 mg/kg ganciclovir every 12 h combined with methylprednisolone (80 mg/day). After 2 weeks of anti-infection treatment, white blood cell counts and PCT levels gradually reduced to normal, as did the oxygenation index. However, the respiratory distress exhibited by the patient could not be relieved, requiring continuous analgesia, sedation and mechanical ventilation.

A large amount of pale-yellow thin secretions was continually aspirated from the lung. CT imaging (Fig. 5C and D) showed that the lung-infiltrating shadow was progressing. However, no pathogens were identified in the subsequent sputum culture (which was repeated nine times) and mNGS (which was repeated twice) of BALF. Specifically, the patient underwent two rounds of BALF mNGS testing since the results of the first test could not explain the pulmonary condition of the patient. BALF was immediately collected for re-testing on the day after the initial results were obtained. However, the two negative results prompted the conclusion that the patient did not have a pulmonary infection, but rather an alternative diagnosis such as SPL. SPL was not confirmed until numerous monoclonal B cells with an abnormal phenotype were identified by MRD in BALF. Subsequently, ~140,000 karyocytes were collected from the BALF, of which 0.28% were monoclonal B cells with an abnormal immunophenotype: $CD19^{dim}$, κ^+, $CD20^+$, $CD45^{dim}$, $CD79b^+$, λ^-, $CD5^-$, $CD10^-$, $CD38^-$, $CD56^-$ and small forward and side scatter (Fig. 6). This profile was consistent with the immunophenotyping results of bone marrow cells (Fig. 7). The antitumor treatment of the patient was ineffective, resulting in mortality due to respiratory failure on day 15 of mechanical ventilation.

Literature review

A combination of search terms (lymphoma and pulmonary infiltrates) was used to screen abstracts and titles under case reports in the PubMed database (https://pubmed.ncbi.nlm.nih.gov/). A total of 386 relevant studies were identified. After evaluating the titles and abstracts, 299 irrelevant reports and duplicate cases were excluded. Within the remaining 87

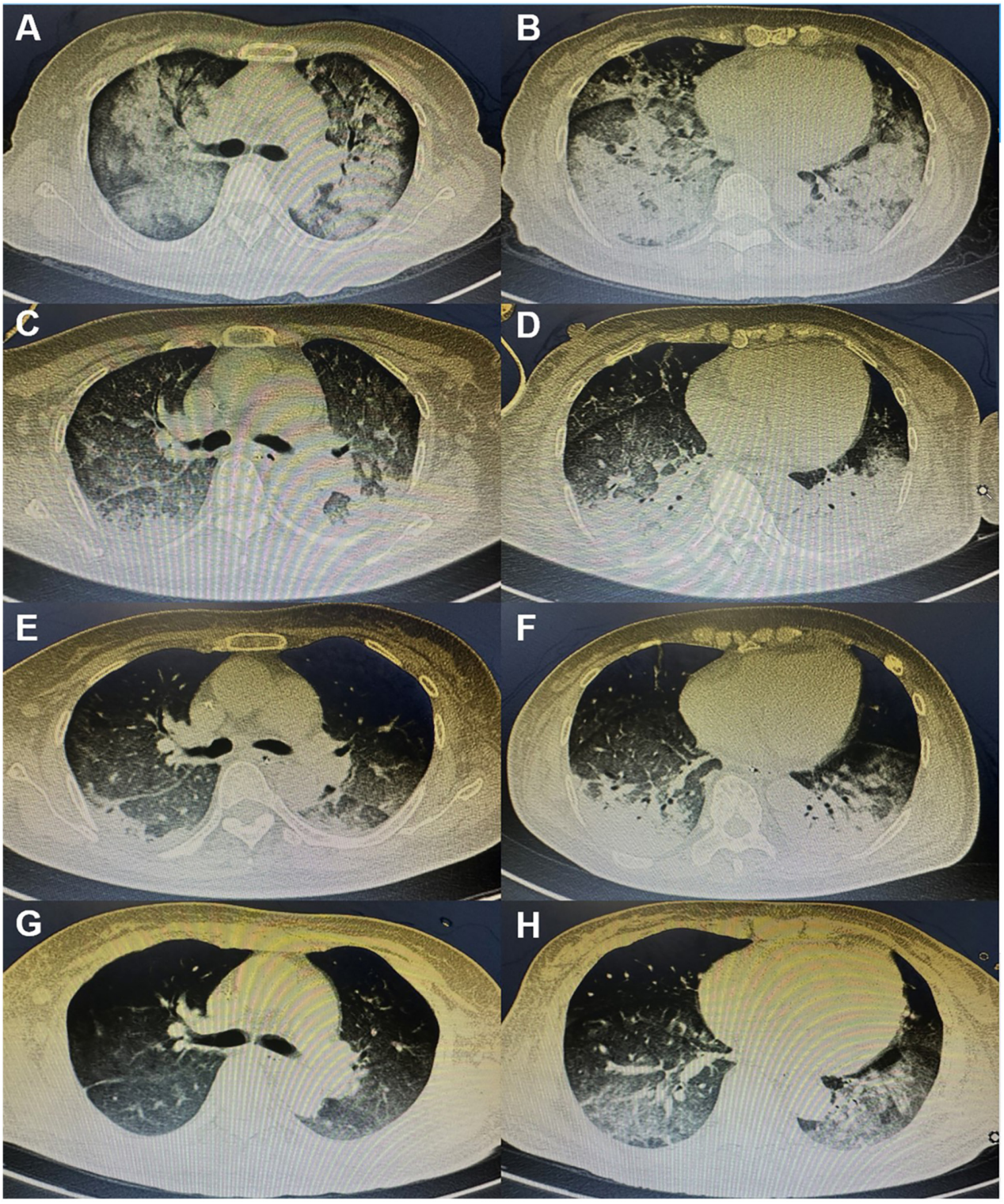

Figure 1. Chest CT scans of the patient in Case 1. (A and B) Chest CT at admission in October 2024: (A) shows the upper lobes of both lungs; (B) shows the lower lobe of the left lung as well as the middle and lower lobes of the right lung. Both revealed large ground-glass opacities, patchy shadows and multiple nodules, as well as enlarged mediastinal lymph nodes. (C and D) Chest CT at discharge in October 2024: (C) shows the upper lobes of both lungs; (D) shows the lower lobe of the left lung as well as the middle and lower lobes of the right lung. Both revealed decreased patchy shadows and multiple nodules. (E and F) Chest CT at admission in November 2024: (E) shows the upper lobes of both lungs; (F) shows the lower lobe of the left lung as well as the middle and lower lobes of the right lung. Both revealed large consolidation, segmental atelectasis and mediastinal lymph nodes. (G and H) Chest CT at discharge in November 2024: (G) shows the upper lobes of both lungs; (H) shows the lower lobe of the left lung as well as the middle and lower lobes of the right lung. Both revealed that the lung disease was locally alleviated.

studies, 56 consisted of primary pulmonary lymphoma and 31 contained SPL. Of these 31 cases, 11 were excluded due to non-English language use or a misdiagnosis of SPL. An additional four were excluded due to being dated before the 21st century. Ultimately, 16 patient case reports were enrolled for analysis (6-21). Fig. 8 exhibits the screening process

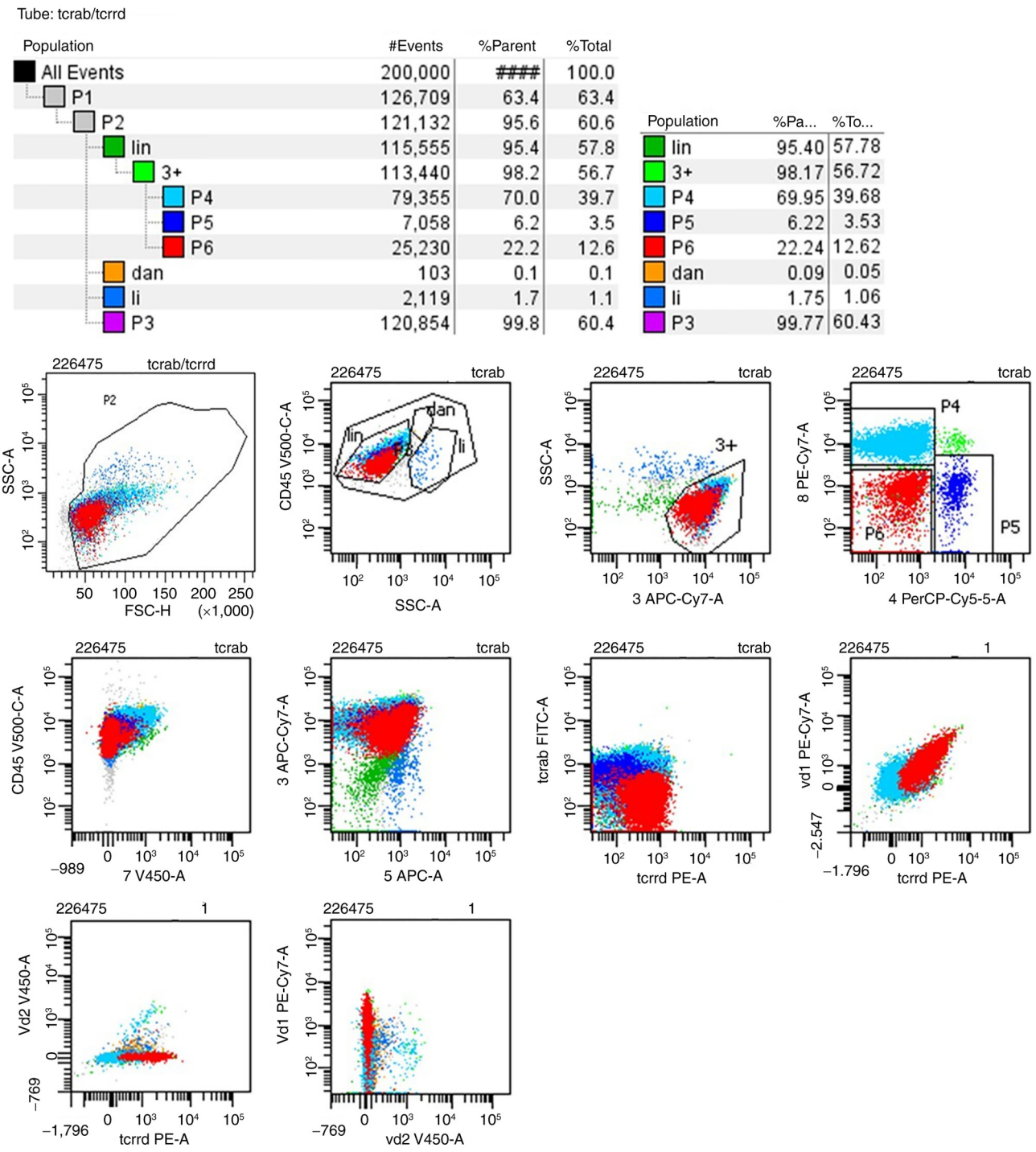

Figure 2. Representative flow cytometry plots of BALF from the patient in Case 1. P1: Cell aggregates were excluded via FSC-H/FSC-A gating; P2: Cell debris was eliminated via SSC-A/FSC-H gating; P3: $CD45^+$ cells; P4: $CD4^-CD8^+$ cells; P5: $CD4^+CD8^-$ cells; P6: $CD4^-CD8^-$ cells; lin: lymphocytes; 3+: $CD3^+$ lymphocytes; dan: monocytes; li: granulocytes. Panel-marker correspondence: Panel 3 (APC-Cy7-A)= CD3; Panel 4 (PerCP-Cy5-5-A)=CD4; Panel 8 (PE-Cy7-A)=CD8; Panel 7 (V450-A)=CD7; Panel 5 (APC-A)=CD5; Panel tcrrd (PE-A)=TCRγδ; Panel tcrab (FITC-A)=TCRαβ; Panel vd1 (PE-Cy7-A)=TCRVδ1; Panel vd2 (V450-A)=TCRVδ2.

and Table I outlines the basic information of 18 patients who experienced SPL (including the 2 cases outlined in the present report).

Within the 18 cases, SPL occurred in individuals of both sexes and varying ages. The ratio of male to female occurrence was 1:1 with a higher frequency among individuals aged >60 years (Table II). The three most prevalent clinical manifestations in these patients were dyspnea (66.7%), cough (33.3%) and a fever (27.8%). These symptoms are consistent with the 2 cases outlined in the present report. However, the patients in the present report manifested a cough with a large amount of pulmonary secretion, but did not exhibit hemoptysis. According to the literature, the proportion of asymptomatic patients was as high as 27.8%. It is worth noting that within these 18 patients, only 2 (11.1%) were associated with pulmonary infection. Among the chest CT findings, the majority

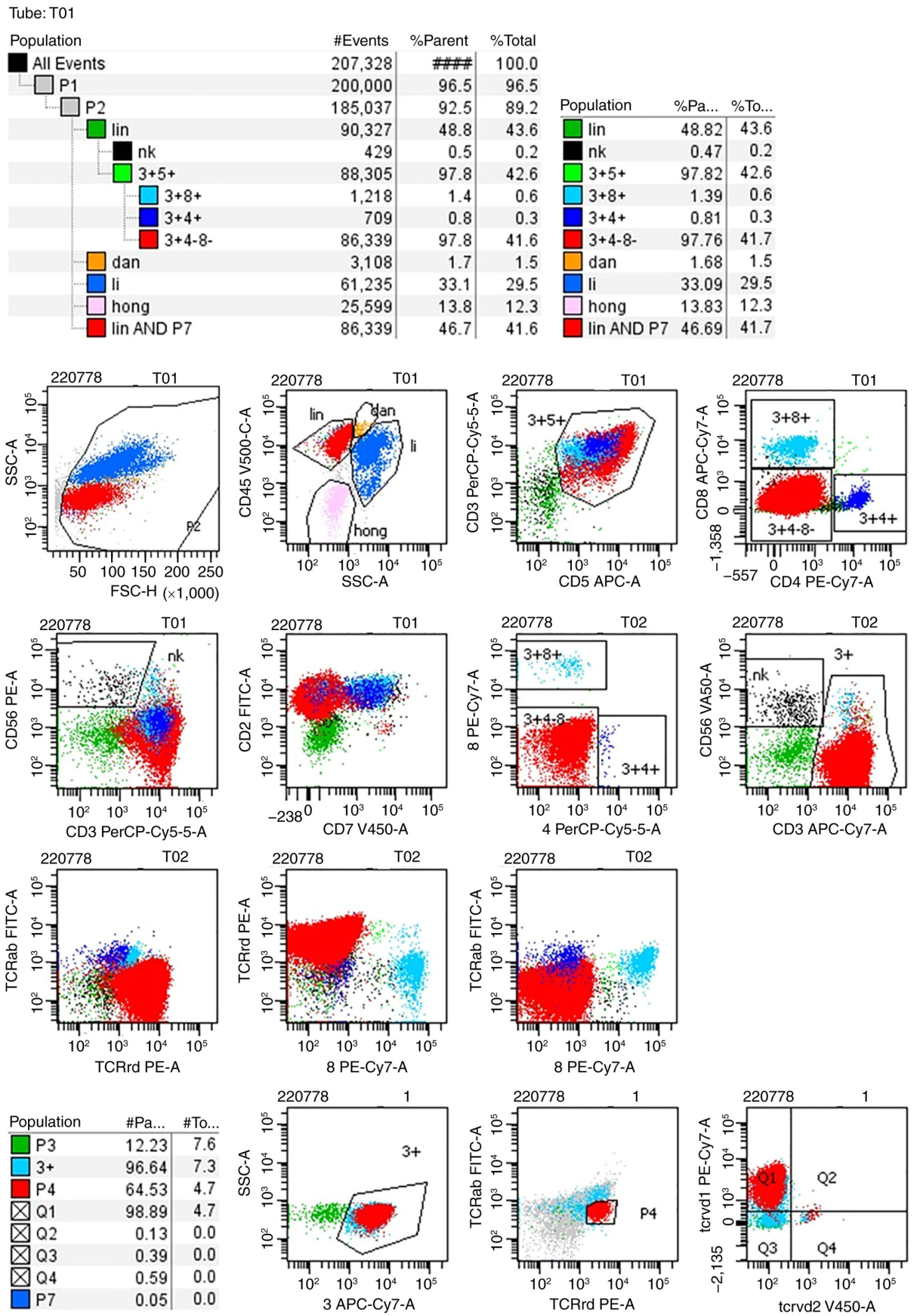

Figure 3. Representative flow cytometry plots of bone marrow from the patient in Case 1. P1: Cell aggregates were excluded via FSC-H/FSC-A gating; P2: Cell debris was eliminated via SSC-A/FSC-H gating; lin: lymphocytes; nk: NK cells; 3+5+: $CD3^+CD5^+$ cells; 3+8+: $CD3^+CD4^-CD8^+$ cells; 3+4+: $CD3^+CD4^+CD8^-$ cells; 3+4-8-: $CD3^+CD4^-CD8^-$ cells; dan: monocytes; li: granulocytes; hong: erythrocytes; lin and P7: $CD3^+CD4^-CD8^-$ cells. Panel-marker correspondence: Panel 3 (APC-Cy7-A)=CD3; Panel 4 (PerCP-Cy5-5-A)=CD4; Panel 8 (PE-Cy7-A)=CD8; Panel TCRrd (PE-A)=TCRγδ; Panel TCRab (FITC-A)=TCRαβ; Panel tcrvd1 (PE-Cy7-A)=TCRVδ1; Panel tcrvd2 (V450-A)=TCRVδ2. Values in the bottom left corner of the figure refer to the quadrants of the plot in the bottom right corner.

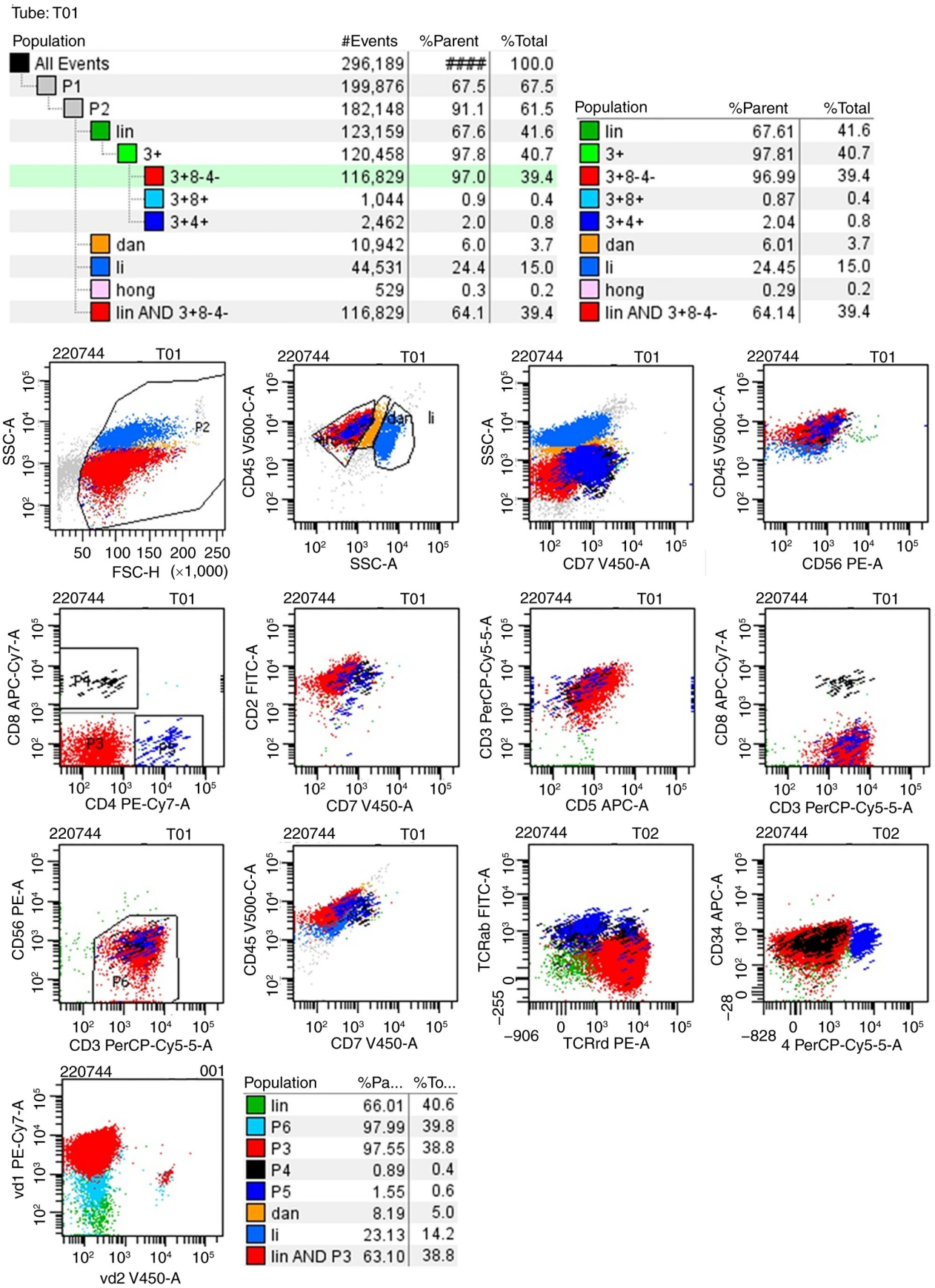

Figure 4. Representative flow cytometry plots of peripheral blood from the patient in Case 1. P1: Cell aggregates were excluded via FSC-H/FSC-A gating; P2: Cell debris was eliminated via SSC-A/FSC-H gating; P3: $CD4^-CD8^-$ cells; P4: $CD4^-CD8^+$ cells; P5: $CD4^+CD8^-$ cells; P6: $CD3^+CD56^-$ cells; lin: lymphocytes; 3+8+: $CD3^+CD4^-CD8^+$ cells; 3+4+: $CD3^+CD4^+CD8^-$ cells; 3+8-4-: $CD3^+CD4^-CD8^-$ cells; dan: monocytes; li: granulocytes; hong: erythrocytes; lin and 3+8-4-: $CD3^+CD4^-CD8^-$ cells; lin and P3: $CD4^-CD8^-$ cells. Panel-marker correspondence: Panel 4 (PerCP-Cy5-5-A)=CD4; Panel TCRrd (PE-A)=TCRγδ; Panel TCRab (FITC-A)=TCRαβ; Panel vd1 (PE-Cy7-A)=TCRVδ1; Panel vd2 (V450-A)=TCRVδ2. Given that the proportion of some cell populations is markedly low, magnifying the cell particles during data analysis resulted in linear shapes rather than dot-like cell clusters.

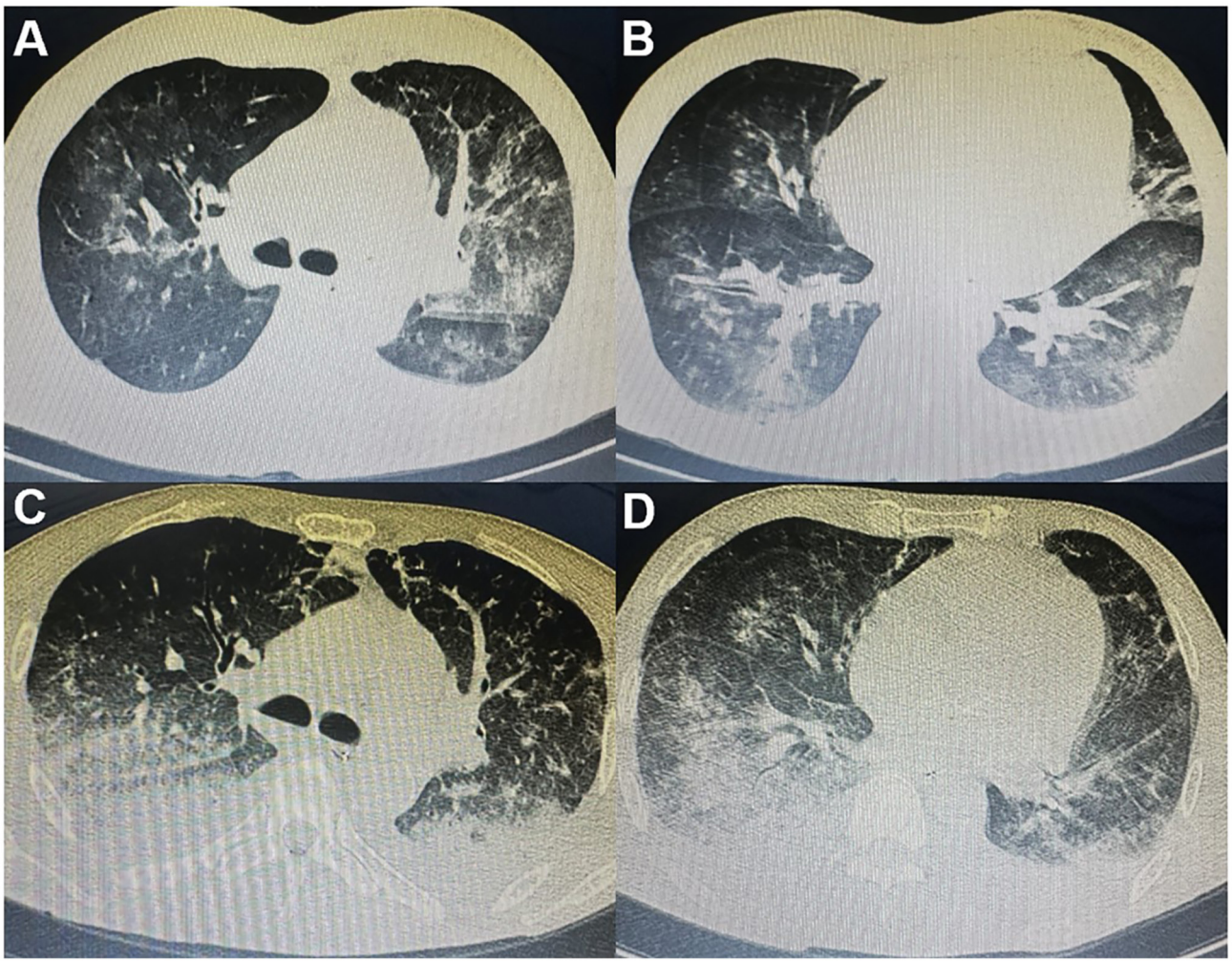

Figure 5. Chest CT scans of the patient in Case 2. (A and B) Chest CT at admission in November 2024: (A) shows the upper lobes of both lungs; (B) shows the lower lobe of the left lung as well as the middle and lower lobes of the right lung. Both revealed large areas of ground-glass opacity and patchy shadows. (C and D) Chest CT at discharge in November 2024: (C) shows the upper lobes of both lungs; (D) shows the lower lobe of the left lung as well as the middle and lower lobes of the right lung. Both revealed that the lung-infiltrating shadow was progressing.

of SPL exhibited bilateral lung infiltration, with only 2 cases showing unilateral infiltration (Table III). The majority of chest imaging findings suggested ground glass density (50%), lymph node enlargement (33.3%), multiple pulmonary nodules (44.4%) and lung consolidation (27.8%). Other presentations included single lymph node enlargement, pleural effusion and cavities.

Pathological characteristics were determined by a pathologist in all 18 cases (Table IV). There were no cases of Hodgkin's lymphoma. However, 4 cases were confirmed to contain diffuse large B cell lymphoma and there were 3 cases of mucosa-associated lymphoid tissue (MALT) and adult T cell lymphoma/leukemia as well as 2 cases of peripheral T cell lymphoma and follicular lymphoma, which were confirmed separately. The remaining cases were confirmed as angioimmunoblastic T cell lymphoma, T-acute lymphoblastic leukemia/lymphoblastic lymphoma, anaplastic large cell lymphoma and chronic lymphocytic leukemia.

There were a number of differential diagnoses of secondary pulmonary infiltration in patients with lymphoma, including SPL, drug-related lung injury, connective tissue disease and pulmonary infections, especially pulmonary fungal infections and tuberculosis. During the diagnostic process, the persistent clinical symptoms and the radiographic manifestations served as key indicators for clinicians to initiate therapeutic interventions. Diagnostic methods often involved numerous types of invasive methods, such as transbronchial lung biopsy (50%), surgery or thoracoscopic lung biopsy (27.8%), autopsy (16.7%) and BALF immunophenotyping test (27.8%) (Table V). On occasion, multiple biopsy methods were involved in the diagnostic process. Furthermore, it was observed that although transbronchial lung biopsy was used more frequently, the success rate was only 55.6%. Almost half of the patients needed to undergo other methods at the same time due to negative pathological findings or suboptimal biopsy specimen quality. In addition, unlike traditional invasive methods, in the present report, lymphoma cells were detected in BALF in only 5 cases, which has rarely been reported before, despite 1 case initially failing to diagnose SPL and requiring surgical biopsy for a definitive answer (case no. 11).

With regard to treatment and prognosis, 7 patients received combination chemotherapy after SPL diagnosis, 2 patients received single-agent chemotherapy with chlorambucil or cladribine respectively, 2 patients received only glucocorticoid

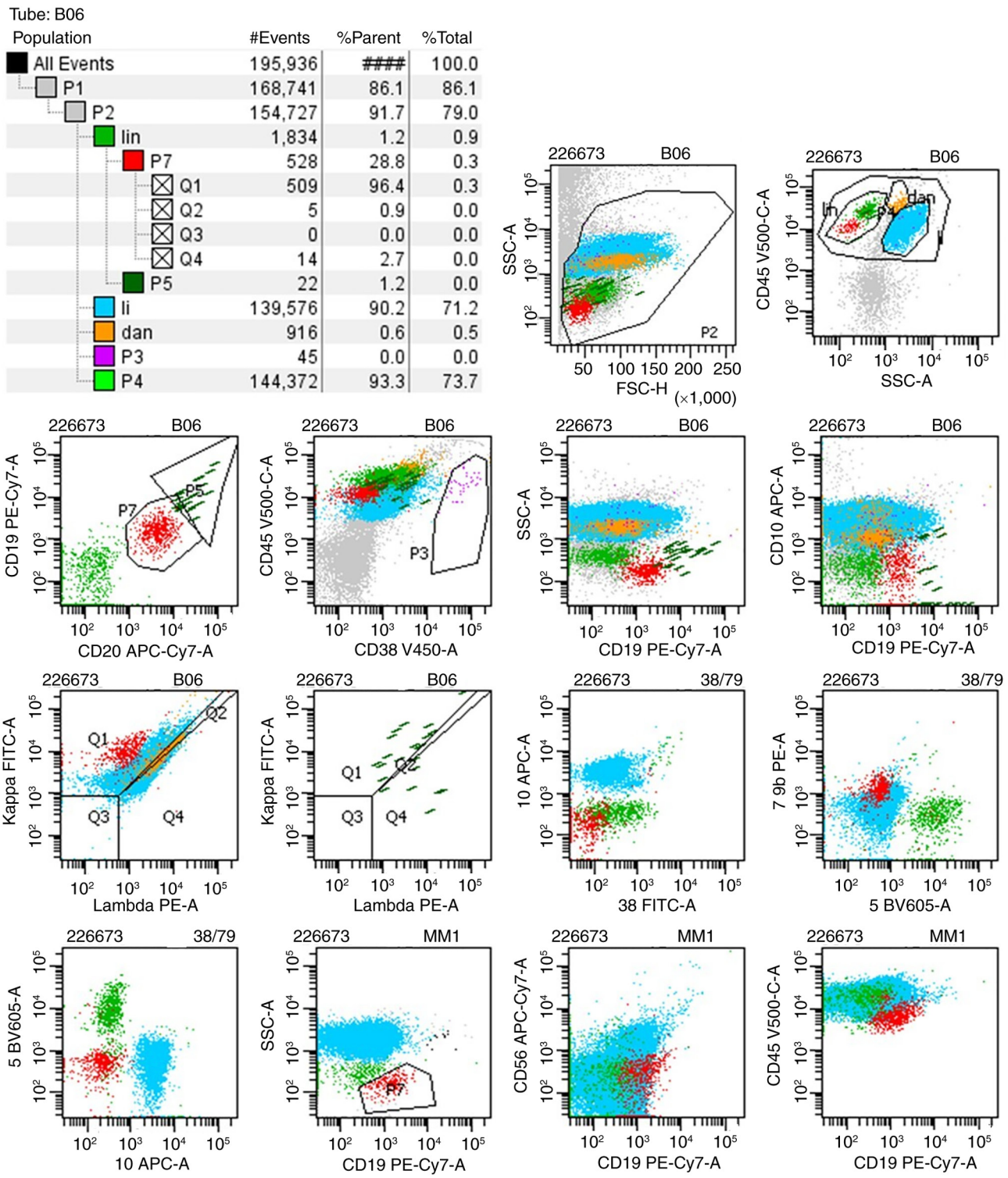

Figure 6. Representative flow cytometry plots of BALF from the patient in Case 2. P1: Cell aggregates were excluded via FSC-H/FSC-A gating; P2: Cell debris was eliminated via SSC-A/FSC-H gating; P3: $CD38^{++}$ plasma cells; P4: $CD45^{+}$ cells; P5: phenotypically normal B cells; P7: phenotypically abnormal monoclonal B cells; lin: lymphocytes; dan: monocytes; li: granulocytes. Panel-marker correspondence: Panel 38 (FITC-A)=CD38; Panel 10 (APC-A)=CD10; Panel 5 (BV605-A)=CD5; Panel 79b (PE-A)=CD79b; Panel 5 (APC-A)=CD5. The two plots labeled 'Kappa FITC-A' and 'Lambda PE-A' are identical. The first plot serves to set the gate using granulocytes as the background, thereby allowing the second plot to clearly determine whether this cell population expresses Kappa or Lambda, and classify this cell population into Q1/Q2/Q3/Q4 based on the results. Given that the proportion of a number of cell populations is markedly low, magnifying the cell particles during data analysis resulted in linear shapes rather than dot-like cell clusters.

therapy, 1 patient received prednisolone followed by allogeneic hematopoietic stem cell transplantation and 4 patients received no treatment or only palliative care. The overall prognosis of SPL was poor, with only 44.6% of enrolled patients exhibiting ongoing survival (Table II). However, early diagnosis and treatment has the potential to improve prognosis. As for the 2 cases outlined in the present report, the first patient, who had just achieved complete remission 2 months prior and

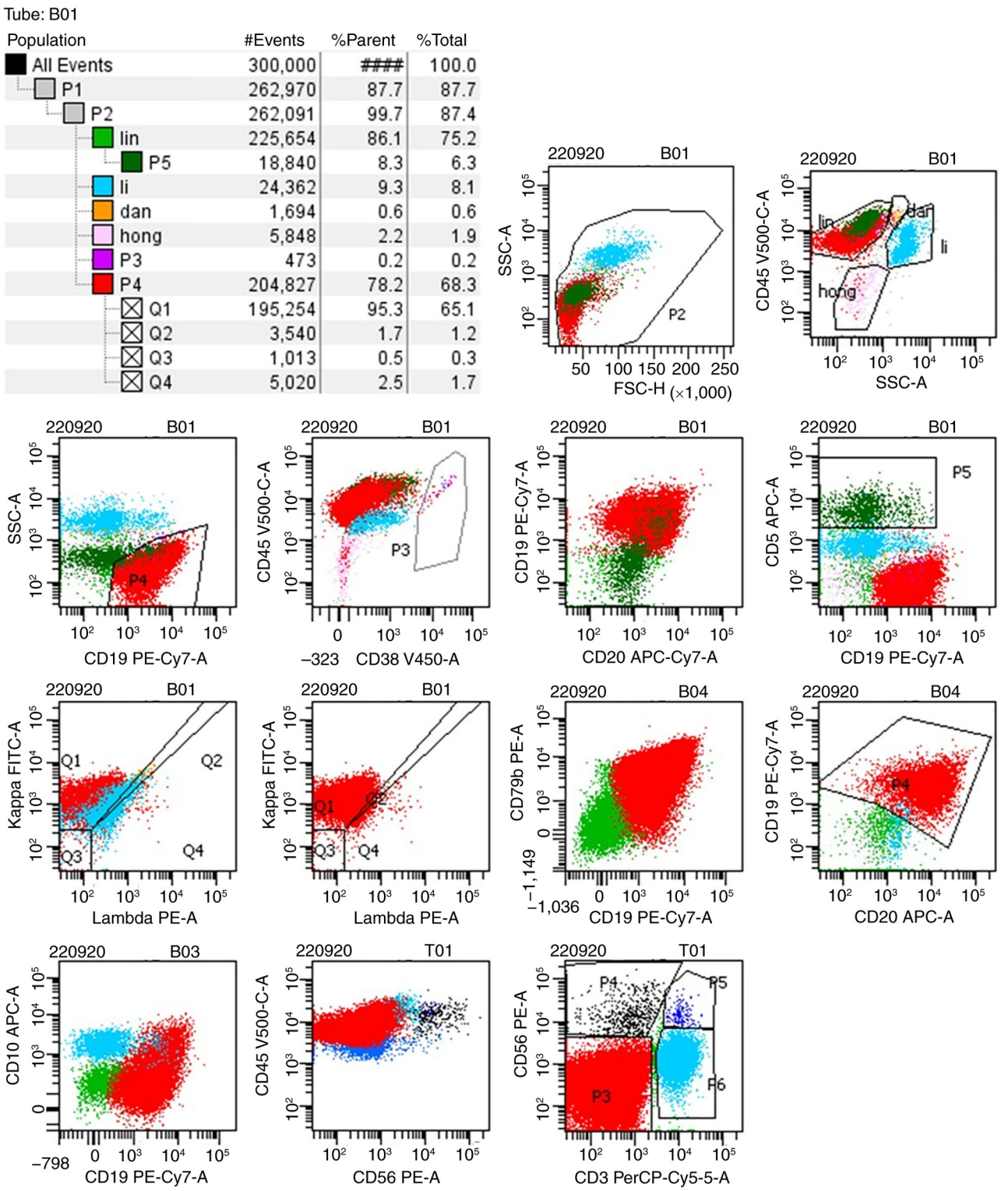

Figure 7. Representative flow cytometry plots of bone marrow from the patient in Case 2. P1: Cell aggregates were excluded via FSC-H/FSC-A gating; P2: Cell debris was eliminated via SSC-A/FSC-H gating; P3: $CD38^{++}$ plasma cells; P4: phenotypically abnormal monoclonal B cells; P5: $CD5^{+}$ T cells; lin: lymphocytes; dan: monocytes; li: granulocytes; hong: erythrocytes. The two plots labeled 'Kappa FITC-A' and 'Lambda PE-A' are identical. The first plot serves to set the gate using granulocytes as the background, thereby allowing the second plot to clearly determine whether this cell population expresses Kappa or Lambda, and classify this cell population into Q1/Q2/Q3/Q4 based on the results.

developed a pulmonary infection during the treatment course of admission, received only methylprednisolone for antitumor therapy. The second patient received antitumor therapy with dexamethasone, cyclophosphamide and bendamustine after admission and continued with methylprednisolone treatment after an SPL diagnosis was confirmed. Both patients eventually progressed rapidly to mortality. The marked differences in treatments among patients may be attributed to individualized risk-benefit assessments based on a number of key factors differing between each patient. These may include disease

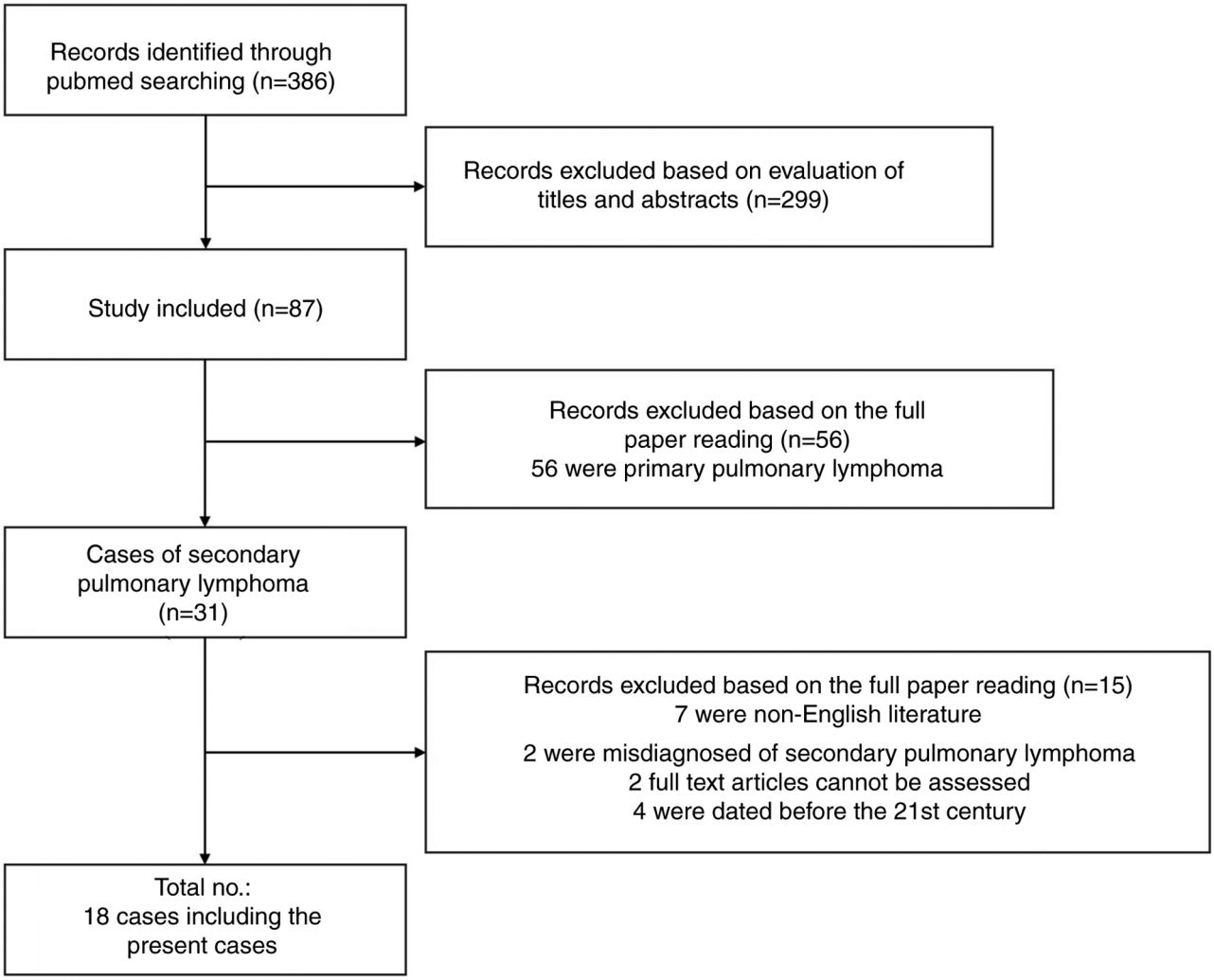

Figure 8. Literature review screening process.

characteristics (pathological confirmation, stage, tumor burden and aggressiveness of the lesion) and patient-specific factors (age, performance status, comorbidities, organ function and previous treatment history). Additionally, the treatment preferences of patients themselves also serve an important role in the selection of treatment regimens. Between the 2 cases in the present report, the first declined following further antitumor treatment. By contrast, the second patient underwent combination chemotherapy immediately upon confirmation of relapsed lymphoma after admission.

Discussion

Within the present report, 2 cases of patients diagnosed with NHL, but having achieved complete remission following CHOP treatment, were outlined. The patients subsequently developed respiratory distress. Due to the pneumonia-like symptoms, signs and chest CT scan findings, the patients were initially diagnosed with pulmonary infection. Following combination treatment with multiple antibiotics, their sputum culture and mNGS of BALF were both negative. However, the patients continued to develop a fever and the imaging findings continued to progress in both lungs. The MRD tests of BALF were performed to establish the existence of SPL. Based on the diagnosis of SPL, a glucocorticoid-based treatment regimen was implemented, a method consistent with a number of reported cases (18,20). However, both patients ultimately succumbed to respiratory failure within 1 month. The lung is a common secondary site of involvement in lymphoma, accounting for ~24% of cases in NHL (22). The clinical symptoms of SPL are non-specific, except for respiratory and extrapulmonary symptoms. However, common symptoms include dyspnea (66.7%), cough (33.3%) and fever (27.8%). The proportion of asymptomatic patients was as high as 27.8% in the reported literature. In previous reports, the imaging findings of SPL have included ground glass density (50%), lymph node enlargement (33.3%), multiple pulmonary nodules (44.4%) and lung consolidation (27.8%). Due to the atypical clinical manifestations, the majority of cases were initially misdiagnosed as tuberculosis, pneumonia or deep fungal infections.

The lung is a predominant site for opportunistic infections. The risk of such infections is determined by the extent of pathogen exposure, host immunological competence and specific pathogen-host interaction mechanisms (4). Among patients with hematological malignancies, pulmonary

Table I. Reported cases of secondary pulmonary lymphoma.

Study no.	First author, year	Age, years	Sex	Lymphoma type	Study title	(Refs.)
1	Miyahara *et al*, 2001	27	F	Diffuse large B cell non-Hodgkin's malignant lymphoma	Pulmonary lymphoma of large B cell type mimicking Wegener's granulomatosis	(6)
2	Wieker *et al*, 2002	63	F	MALT-lymphoma	Pulmonary low-grade MALT-lymphoma associated with localized pulmonary amyloidosis. A case report	(7)
3	Kusumoto *et al*, 2004	35	F	MALT-lymphoma	T(11;18)-bearing pulmonary mucosa-associated lymphoid tissue lymphoma responding to cladribine	(8)
4	Fujisawa *et al*, 2007	62	M	Peripheral T cell lymphoma	Peripheral T cell lymphoma with diffuse pulmonary infiltration and an increase in serum KL-6 level	(9)
5	Jankipersadsing *et al*, 2007	49	F	Adult T cell leukemia/lymphoma	Spontaneous regression of pulmonary infiltration of adult T cell leukemia/lymphoma	(10)
6	Hosseinnezhad *et al*, 2011	82	M	Chronic lymphocytic leukemia	Diffuse pulmonary infiltrates in an old man with chronic lymphocytic leukemia	(11)
7	Samiullah *et al*, 2014	60	M	MALT-lymphoma	Metastatic gastric MALT lymphoma masquerading as pulmonary infiltrates, with a dramatic response to chemotherapy	(12)
8	Sedgwick *et al*, 2015	81	F	Anaplastic large cell lymphoma	Lesson of the month 1: A rash decision	(13)
9	Suzuki *et al*, 2017	63	M	Diffuse large B cell lymphoma	EBV-positive diffuse large B cell lymphoma as a secondary malignancy arising in a myelodysplastic syndrome patient who was treated with azacitidine	(14)
10	Kajimoto *et al*, 2020	53	F	Diffuse large B cell lymphoma + T cell lymphoma	T cell lymphoma with a granulomatous lesion of the lungs after autologous hematopoietic stem cell transplantation for Epstein-Barr virus-positive diffuse large B cell lymphoma: A unique rare case of metachronous B cell and T cell lymphoma	(15)
11	Yagyu *et al*, 2020	82	F	Follicular lymphoma	Malignant lymphoma mimics miliary tuberculosis by diffuse micronodular radiographic findings	(16)
12	Miyaoka *et al*, 2020	39	M	T-acute lymphoblastic leukaemia/ lymphoblastic lymphoma	Aggressive lung involvement in a patient with T-acute lymphoblastic leukaemia/lymphoblastic lymphoma: A tricky and rare case report	(17)
13	Tanaka *et al*, 2022	69	M	Intravascular large B cell lymphoma	Rapid deterioration of intravascular large B cell lymphoma with mass formation in the trigeminal nerve and multiple organ infiltration: An autopsy case report	(18)
14	Kobe *et al*, 2022	79	F	Adult T cell lymphoma/leukaemia	Cryobiopsy for *Pneumocystis jirovecii* pneumonia secondary to adult T cell lymphoma/leukaemia	(19)

Table I. Continued.

Study no.	First author, year	Age, years	Sex	Lymphoma type	Study title	(Refs.)
15	Yamamoto *et al*, 2022	73	M	Angioimmunoblastic T cell lymphoma	Use of bronchoalveolar lavage in diagnosing angioimmunoblastic T cell lymphoma: A case report	(20)
16	Tanaka *et al*, 2022	76	M	Intestinal T cell lymphoma	Intestinal T cell lymphoma with lung and lymph node involvement at relapse	(21)
17	The present study	63	F	Peripheral T cell lymphoma	Secondary pulmonary lymphoma diagnosed by minimal residual disease detected in bronchoalveolar lavage fluid: A case report	-
18	The present study	59	M	Follicular lymphoma	Secondary pulmonary lymphoma diagnosed by minimal residual disease detected in bronchoalveolar lavage fluid: A case report	-

BALF, bronchoalveolar lavage fluid; F, female; M, male; MALT, mucosa-associated lymphoid tissue; KL-6, Krebs von den Lungen-6; EBV, Epstein-Barr virus.

Table II. Analysis of information regarding lung infiltration secondary to lymphoma.

Feature	Cases, n (%)
Age, years	
≤60	7 (38.9)
>60	11 (61.1)
Sex	
Male	9 (50.0)
Female	9 (50.0)
Respiratory symptoms	
Asymptomatic	5 (27.8)
Cough	6 (33.3)
Dyspnea	12 (66.7)
Fever	5 (27.8)
Hemoptysis	2 (11.1)
Chest pain	0 (0.0)
Coexisting with pulmonary infection	2 (11.1)
Outcome	
Remission	8 (44.4)
Mortality	10 (55.6)

Table III. Imaging features of the chest.

Feature	Cases, n (%)
Bilateral disease	16 (88.9)
Unilateral disease	2 (11.1)
Ground glass opacity	9 (50.0)
Consolidation	5 (27.8)
Single nodule or mass	1 (5.6)
Multiple nodules	8 (44.4)
Pleural effusion	3 (16.7)
Lymphadenopathy	6 (33.3)
Cavity	1 (5.6)

opportunistic infections deteriorate rapidly and evolve into respiratory failure. In the cases outlined in the present report, infection was initially suspected based on sputum culture and mNGS results of BALF, which revealed a number of opportunistic pathogens. Following anti-infective treatment, the clinical manifestations of the patients showed marked improvement during the initial phase of treatment. No pathogens were found in the subsequent sputum culture and mNGS of BALF. However, the symptoms exhibited by the patients and the imaging findings worsened afterwards, which prompted an alternative diagnosis. Regardless of the ultimate etiology, prompt definitive diagnosis and targeted therapeutic intervention are key in optimizing clinical outcomes.

Histopathological workup is often required to establish a correct diagnosis. In current clinical practice, the diagnostic evaluation of pulmonary lesions primarily relies on minimally

Table IV. Pathological types of the 18 cases.

Pathological type	Cases, n (%)
Hodgkin's lymphoma	0 (0.0)
Mucosa-associated lymphoid tissue	3 (16.7)
Diffuse large B cell lymphoma	4 (22.2)
Angioimmunoblastic T cell lymphoma	1 (5.6)
Peripheral T cell lymphoma	2 (11.1)
Adult T cell lymphoma/leukemia	3 (16.7)
Follicular lymphoma	2 (11.1)
T-acute lymphoblastic leukemia/ lymphoblastic lymphoma	1 (5.6)
Anaplastic large cell lymphoma	1 (5.6)
Chronic lymphocytic leukemia	1 (5.6)

Table V. Diagnostic methods and accuracy of the diagnosis process.

Diagnostic method	Cases, n (%)	Success rate, %
CT-guided percutaneous lung biopsy	0 (0.0)	0.0
Transbronchial lung biopsy	9 (50.0)	55.6
Surgery or thoracoscopy lung biopsy	5 (27.8)	100.0
Autopsy	3 (16.7)	100.0
Bronchoalveolar lavage fluid	5 (27.8)	80.0

invasive techniques, such as bronchoscopy and CT-guided percutaneous lung biopsy, thereby markedly reducing the need for more invasive surgical interventions (23-25). However, it has been established that, although transbronchial lung biopsy is conducted more frequently, the success rate lies at only 55.6%. Furthermore, although surgical lung biopsy and autopsy often achieve an approximate diagnostic success rate of 100%, both are associated with notably higher risks and cost, given that a lung biopsy is often difficult to perform and requires patient cooperation. In hematological patients, such as patients with thrombocytopenia and coagulation disorders, these procedures may notably increase the risk of complications associated with invasive diagnostic interventions, and when sedation or general anesthesia is required, patients are exposed to additional risks. The literature demonstrates that a total of 27.8% of patients underwent surgery or thoracoscopic lung biopsy. Therefore, non-invasive tools to improve the differentiation of unclear pulmonary lesions are desirable.

Regarding diagnostic choices for the included cases from the literatures, the majority of patients underwent biopsy procedures, including repeated transbronchial lung biopsy, surgical lung biopsies and autopsies (Table V). Immunohistochemical analysis of BALF was conducted in only 5 patients. Of these, 4 patients were directly diagnosed through BALF immunohistochemistry, while the remaining patient still required surgical biopsy for definitive diagnosis of SPL. This corresponds with a diagnostic success rate of only 80% for BALF immunohistochemistry. Biopsy is the well-established standard for diagnosis, but if lymphoma cells can be identified through simple flow cytometry-based immunohistochemistry of BALF, this would potentially spare patients from the discomfort and risks associated with invasive biopsies. For the 2 patients in the present report who did not undergo biopsy, the lymphoma clinicians had initially planned CT-guided lung biopsies. However, both patients exhibited marked coagulation abnormalities and low oxygenation indices, rendering the procedure too high-risk. Ultimately, the clinicians decided against biopsy; therefore, to confirm the diagnosis, alternative approaches had to be explored. Both of the cases presented in the present study happened to produce large amounts of daily secretion from the lungs, prompting the collection of BALF for relevant diagnostic tests.

Flow cytometry analysis (Table SII) of the alveolar cell composition in BALF, particularly the percentages of $CD4^+$ and $CD8^+$ T cells, has long been applied in the diagnosis of diseases, including hypersensitivity pneumonitis, idiopathic non-specific interstitial pneumonia, idiopathic pleuroparenchymal fibroelastosis and unclassifiable idiopathic interstitial pneumonia (26). It may also predict the progression and prognosis of fibrotic diseases such as interstitial lung disease (27). Additionally, literature has reported that flow cytometry-based analysis of inflammatory cells in BALF can be indirectly used to assess the degree of lung tissue damage and macrophage subtyping to evaluate the pulmonary immune status (28). The use of flow cytometry depends on the selection of antigens. In the majority of lymphoproliferative disorders, lymphocyte subset analysis of BALF demonstrates a T cell predominance (>90%) with fewer B cell populations (<10%). Of note, lymphocytic alveolitis is a characteristic feature of pulmonary lymphoma, which can be examined by BALF cytological analysis (29). Particularly in pulmonary B cell lymphomas, flow cytometry of BALF has revealed both a notable elevation in B cell proportion (>10%) and immunophenotypic evidence of clonal proliferation, which may contribute to a diagnosis (30,31). Similar findings have been observed in pulmonary T cell lymphomas (32).

The basic principle of flow cytometry has been described for multiple purposes, including MRD detection, primarily depending on the selection of antibodies labelled with immunofluorescence (33). MRD testing is a diagnostic tool for patients with hematological diseases, mainly those with acute myeloid leukemia (AML). It refers to the small number of residual leukemia cells in patients with newly diagnosed or refractory/relapsed disease after achieving complete hematological remission through treatment. This encompasses the specific expertise in multiparameter flow cytometry (MFC)-based MRD, molecular MRD, NGS and clinical considerations. Methods for MRD detection using MFC include leukemia-associated immunophenotype (LAIP) and 'different from normal' (D-F-N) approaches. The former involves identifying the LAIP of the patient at initial diagnosis and using it for subsequent MRD monitoring during treatment. The latter is applicable to patients lacking an initial LAIP and can also detect antigen shift occurring during treatment. The combination of LAIP and D-F-N is suitable for both patients without an initial LAIP and for detecting newly emerging phenotypic abnormalities or antigen shift of existing LAIP (34).

With regard to antibody selection, experts from diagnostic groups (34) recommend using MFC with ≥8-color fluorescence labeling for MRD detection to improve specificity. The antibody panels for MRD detection include: i) Core antibodies CD45, CD117, CD34, CD13 and CD33; ii) other antibodies including CD4, CD11b, CD14, CD64 and human leukocyte antigen-DR to assess MRD in monocytic or myelomonocytic AML; iii) CD7, CD19 and CD56 to evaluate cross-lineage antigen expression; and iv) CD133, CD38 and CD123 to detect leukemia stem/progenitor cells. A number of different marker panels have been used to assess MRD. To minimize the number of panels employed, experts recommend (35) the design and validation of a single common panel assay for all MRD studies. Each center should select the appropriate antibody panel for MRD detection based on the disease subtype. For the 2 cases outlined in the present report, both patients underwent bone marrow flow immunophenotyping prior to BALF MRD detection. Therefore, the BALF MRD detection in both cases was performed using fluorochrome-conjugated antibodies specifically tailored to their baseline B cell or T cell lineage.

Among the numerous cases of SPL diagnosed through BALF reported in the literature, only 1 case was found to be confirmed using flow cytometry of BALF, which showed λ-restricted B cells with dim CD20 expression and co-expression of CD5 and CD23, consistent with chronic lymphocytic leukemia. The majority of cases are still diagnosed based on the fractionation results of lymphocytes and neutrophils, cytological findings, combined with clinical characteristics and other biopsy data. Therefore, to the best of our knowledge, the present study was the first to report an SPL diagnosis that relied on MRD testing in BALF. The premise of this examination was that there must be sufficient living cells in BALF for detection. Overall, the minimum number of cells needed for accurate reporting of MRD is 500,000-1,000,000 excluding $CD45^-$ cells and debris (35). These high numbers enable the assessment of possible MRD <0.1%. Furthermore, except for the definite MRD cell population identified during specimen collection, other residual leukemia cell subsets must be confirmed by skilled operators or personnel with professional knowledge of flow cytometry. However, in the cases outlined in the preset report, only 140,000 nucleated cells were found in Case 2 and even fewer in Case 1, but a positive status was still exhibited based on the 0.1% threshold.

To provide guidance for early detection and diagnosis, the present report recommends the following clinical strategies: i) In patients with a prior confirmed diagnosis of NHL, when respiratory symptoms emerge, the possibility of secondary pulmonary infection and SPL should both be considered in the differential diagnosis; ii) when chest CT reveals pneumonia-like changes, differentiating SPL from pneumonia is challenging, therefore a comprehensive evaluation incorporating bronchoalveolar lavage, serum testing and tissue biopsy is advised when necessary; and iii) in certain cases, if pathological tissue biopsy cannot be performed, MRD detection of BALF can serve as an alternative diagnostic method.

The present study has certain limitations. First, only 2 cases were reported in this study. From these, 1 patient did not receive standardized treatment due to personal reasons, thereby weakening the reliability and statistical power of the study results. Second, the generalizability of the study conclusions is limited as MRD detection in BALF requires collecting a sufficient number of cells for staining, and most patients may not meet this criterion. Third, this study excluded cases before the 21st century, which may introduce temporal selection bias. However, cases before the 21st century are relatively rare, which may mitigate this type of bias.

Acknowledgements

The authors would like to thank the Hematology and Cytology Laboratory of Wuhan Union Hospital for performing all the flow cytometry assays and Weiyuan Gene Technology Co., Ltd., for performing all the NGS tests.

Funding

The present report was supported by The Project of Department of Science and Technology of Hubei Province (grant no. 2024AFB690).

Availability of data and materials

The data generated in the present study may be found in the National Center for Biotechnology Information sequence read archive under accession number PRJNA1363855 or at the following URL: https://www.ncbi.nlm.nih.gov/bioproject/PRJNA1363855.

Authors' contributions

YH and ZL contributed towards drafting and revising the manuscript, as well as gathering the experimental data. LR and XZ analyzed and interpreted the data. HL served a key role in developing the conceptual framework and methodological approach of the present report. YY was involved in study conceptualization and oversight, taking lead responsibility for critically revising the intellectual content of the manuscript. All authors read and approved the final version of the manuscript. YH, ZL and YY confirm the authenticity of all the raw data.

Ethics approval and consent to participate

As a retrospective analysis, the present report obtained an informed consent waiver with oversight and approval from the Institutional Review Board at Union Hospital, Tongji Medical College, Huazhong University of Science and Technology (Wuhan, Hebei). No ethics approval number was obtained.

Patient consent for publication

Written informed consent was obtained from the patients' spouses for publication of all images and clinical data in the present case report.

Competing interests

The authors declare that they have no competing interests.

References

1. Jaffe ES: Diagnosis and classification of lymphoma: Impact of technical advances. Semin Hematol 56: 30-36, 2019.
2. Berkman N, Breuer R, Kramer MR and Polliack A: Pulmonary involvement in lymphoma. Leuk Lymphoma 20: 229-237, 1996.
3. Zhang MC, Zhou M, Song Q, Wang S, Shi Q, Wang L, Yan FH, Qu JM and Zhao WL: Clinical features and outcomes of pulmonary lymphoma: A single center experience of 180 cases. Lung Cancer 132: 39-44, 2019.
4. Kumar R and Ison MG: Opportunistic infections in transplant patients. Infect Dis Clin North Am 33: 1143-1157, 2019.
5. Shao L, Jiang L, Wu S, Yu L, Wang L and Huang X: Simultaneous occurrence of invasive pulmonary aspergillosis and diffuse large B-cell lymphoma: Case report and literature review. BMC Cancer 20: 15, 2020.
6. Miyahara N, Eda R, Umemori Y, Murakami T, Kunichika N, Makihata K, Aoe K, Murakami K, Takeyama H and Harada M: Pulmonary lymphoma of large B-cell type mimicking Wegener's granulomatosis. Intern Med 40: 786-790, 2001.
7. Wieker K, Röcken C, Koenigsmann M, Roessner A and Franke A: Pulmonary low-grade MALT-lymphoma associated with localized pulmonary amyloidosis. A case report. Amyloid 9: 190-193, 2002.
8. Kusumoto S, Kobayashi Y, Tanimoto TE, Hasegawa T, Yokota Y, Tanimoto K, Sekiguchi N, Narabayashi M, Watanabe T, Matsuno Y and Tobinai K: T(11;18)-bearing pulmonary mucosa-associated lymphoid tissue lymphoma responding to cladribine. Int J Hematol 80: 70-74, 2004.
9. Fujisawa T, Suda T, Matsuura S, Enomoto N, Takeshita K, Ohnishi K and Chida K: Peripheral T-cell lymphoma with diffuse pulmonary infiltration and an increase in serum KL-6 level. Respirology 12: 452-454, 2007.
10. Jankipersadsing V, Tauchi T, Ohyashiki K, Tanaka Y, Setoguchi Y and Mukai K: Spontaneous regression of pulmonary infiltration of adult T-cell leukemia/lymphoma. Int J Hematol 86: 207, 2007.
11. Hosseinnezhad A, Seguel JM and Villanueva AG: Diffuse pulmonary infiltrates in an old man with chronic lymphocytic leukemia. Clin Pract 1: e41, 2011.
12. Samiullah S, Bhurgri H, Tufail M, Samad F, Patel S, Marium M, Pliner L, Brelvi Z and Wang W: Metastatic gastric MALT lymphoma masquerading as pulmonary infiltrates, with a dramatic response to chemotherapy. J Gastrointest Cancer 45 (Suppl 1): S151-S154, 2014.
13. Sedgwick CL, Hall PE, Ratnarajah A, Natkunarajah J and Hogh L: Lesson of the month 1: A rash decision. Clin Med (Lond) 15: 206-207, 2015.
14. Suzuki N, Hiraga J, Kato H, Takagi Y, Ujihira N, Narita M and Kagami Y: EBV-positive diffuse large B-cell Lymphoma as a secondary malignancy arising in a myelodysplastic syndrome patient who was treated with azacitidine. Intern Med 56: 1711-1713, 2017.
15. Kajimoto Y, Terasaki Y, Terasaki M, Kunugi S, Okabe Y, Wakita S, Inokuchi K and Shimizu A: T-cell lymphoma with a granulomatous lesion of the lungs after autologous hematopoietic stem cell transplantation for Epstein-Barr virus-positive diffuse large B-cell lymphoma: A unique rare case of metachronous B-cell and T-cell lymphoma. Diagn Pathol 15: 125, 2020.
16. Yagyu K, Kobayashi M, Ueda T, Uenishi R, Nakatsuji Y and Matsushita H: Malignant lymphoma mimics miliary tuberculosis by diffuse micronodular radiographic findings. Respir Med Case Rep 31: 101239, 2020.
17. Miyaoka C, Saraya T, Honda K, Fujiwara M, Ishii H and Takizawa H: Aggressive lung involvement in a patient with T-acute lymphoblastic leukaemia/lymphoblastic lymphoma: A tricky and rare case report. Respirol Case Rep 8: e00614, 2020.
18. Tanaka Y, Momose S, Takayanagi N, Tabayashi T, Tokuhira M, Tamaru JI and Kizaki M: Rapid deterioration of intravascular large B-cell lymphoma with mass formation in the trigeminal nerve and multiple organ infiltration: An autopsy case report. J Clin Exp Hematop 62: 41-45, 2022.
19. Kobe H, Saito K, Arita M and Ishida T: Cryobiopsy for *Pneumocystis jirovecii* pneumonia secondary to adult T-cell lymphoma/leukaemia. Respirol Case Rep 10: e0893, 2021.
20. Yamamoto G, Takamura K, Ishida Y, Sato Y, Sinozaki A, Kikuchi H, Yamamoto M, Kobayashi H, Hirose N and Kikuchi K: Use of bronchoalveolar lavage in diagnosing angioimmunoblastic T-cell lymphoma: A case report. Respirol Case Rep 10: e0924, 2022.
21. Tanaka Y, Mishina T, Miyoshi H, Ohshima K and Nohgawa M: Intestinal T-cell lymphoma with lung and lymph node involvement at relapse. J Med Cases 13: 15-20, 2022.
22. William J, Variakojis D, Yeldandi A and Raparia K: Lymphoproliferative neoplasms of the lung: A review. Arch Pathol Lab Med 137: 382-391, 2013.
23. Borie R, Wislez M, Antoine M, Copie-Bergman C, Thieblemont C and Cadranel J: Pulmonary mucosa-associated lymphoid tissue lymphoma revisited. Eur Respir J 47: 1244-1260, 2016.
24. Swerdlow SH, Campo E, Pileri SA, Harris NL, Stein H, Siebert R, Advani R, Ghielmini M, Salles GA, Zelenetz AD and Jaffe ES: The 2016 revision of the World Health Organization classification of lymphoid neoplasms. Blood 127: 2375-2390, 2016.
25. Zhu M, Chang Y, Fan H, Shi J, Zhu B and Mai X: Primary pulmonary intravascular large B-cell lymphoma misdiagnosed as pneumonia: Four case reports and a literature review. Oncol Lett 25: 234, 2023.
26. Yamagata A, Arita M, Tachibana H, Tokioka F, Sugimoto C, Sumikawa H, Tanaka T, Yasui H, Fujisawa T, Nakamura Y, *et al*: Impact of bronchoalveolar lavage lymphocytosis on the effects of anti-inflammatory therapy in idiopathic non-specific interstitial pneumonia, idiopathic pleuroparenchymal fibroelastosis, and unclassifiable idiopathic interstitial pneumonia. Respir Res 22: 115, 2021.
27. Simons IA, Boerrigter BG, Hovestadt MCM, Mooij-Kalverda KA, Zhang S, Boers LS, van der Zee AHM, Nossent EJ and Duitman JW: Alveolar cell composition in interstitial lung disease and the development of a pulmonary progressive fibrosing phenotype: A retrospective cohort study. Respir Res 26: 164, 2025.
28. Kwiecień I, Rutkowska E, Raniszewska A, Rzeszotarska A, Polubiec-Kownacka M, Domagała-Kulawik J, Korsak J and Rzepecki P: Flow cytometric analysis of macrophages and cytokines profile in the bronchoalveolar lavage fluid in patients with lung cancer. Cancers (Basel) 15: 5175, 2023.
29. Drent M, Wagenaar SS, Mulder PH, van Velzen-Blad H, Diamant M and van den Bosch JM: Bronchoalveolar lavage fluid profiles in sarcoidosis, tuberculosis, and non-Hodgkin's and Hodgkin's disease. An evaluation of differences. Chest 105: 514-519, 1994.
30. Borie R, Wislez M, Antoine M, Fleury-Feith J, Thabut G, Crestani B, Monnet I, Nunes H, Delfau-Larue MH and Cadranel J: Clonality and phenotyping analysis of alveolar lymphocytes is suggestive of pulmonary MALT lymphoma. Respir Med 105: 1231-1237, 2011.
31. Philippe B, Delfau-Larue MH, Epardeau B, Autran B, Clauvel JP, Farcet JP and Couderc LJ: B-cell pulmonary lymphoma: Gene rearrangement analysis of bronchoalveolar lymphocytes by polymerase chain reaction. Chest 115: 1242-1247, 1999.
32. Hanaka M, Yatera K, Itoh C, Kawanami T, Nakanishi T, Katsuragi T, Shimajiri S, Ishimoto H, Tsukada J and Mukae H: Case of adult T-cell leukemia/lymphoma with rapid progression of pulmonary areas of ground-glass attenuation and multiple nodules. Respir Investig 51: 40-45, 2013.
33. Kalina T, Flores-Montero J, van der Velden VH, Martin-Ayuso M, Böttcher S, Ritgen M, Almeida J, Lhermitte L, Asnafi V, Mendonça A, *et al*: EuroFlow standardization of flow cytometer instrument settings and immunophenotyping protocols. Leukemia 26: 1986-2010, 2012.
34. Heuser M, Freeman SD, Ossenkoppele GJ, Buccisano F, Hourigan CS, Ngai LL, Tettero JM, Bachas C, Baer C, Béné MC, *et al*: 2021 Update on MRD in acute myeloid leukemia: A consensus document from the European LeukemiaNet MRD working party. Blood 138: 2753-2767, 2021.
35. Schuurhuis GJ, Heuser M, Freeman S, Béné MC, Buccisano F, Cloos J, Grimwade D, Haferlach T, Hills RK, Hourigan CS, *et al*: Minimal/measurable residual disease in AML: A consensus document from the European LeukemiaNet MRD working party. Blood 131: 1275-1291, 2018.